



# Pump-probe phase spectroscopy with submilliradian sensitivity and nanosecond time delay using Michelson interferometers

C. D. CRUZ,<sup>1</sup> J. C. STEPHENSON,<sup>2</sup> S. ENGMANN,<sup>2,3</sup> E. G. BITTLE,<sup>1</sup>  
AND J. K. WAHLSTRAND<sup>1,\*</sup> 

<sup>1</sup>Physical Measurement Laboratory, National Institute of Standards and Technology, Gaithersburg, MD 20899, USA

<sup>2</sup>Associate, Physical Measurement Laboratory, National Institute of Standards and Technology, Gaithersburg, MD 20899, USA

<sup>3</sup>Theiss Research, La Jolla, CA 92037, USA

\*jared.wahlstrand@nist.gov

**Abstract:** Using two Michelson interferometers, we describe an experimental scheme for sensitive pump-probe spectral interferometry measurements at long time delays. It has practical advantages over the Sagnac interferometer method typically used when long-time delays are required. First, with the Sagnac interferometer, achieving many nanosecond delays requires expanding the size of the interferometer so that the reference pulse arrives before the probe pulse. Because the two pulses still pass through the same region of the sample, long-lived effects can still affect the measurement. In our scheme, the probe and reference pulses are spatially separated at the sample, alleviating the need for a large interferometer. Second, in our scheme, a fixed delay between probe and reference pulses is straightforward to produce and is continuously adjustable while maintaining alignment. Two applications are demonstrated. First, transient phase spectra are presented in a thin tetracene film with up to 5 ns probe delay. Second, impulsive stimulated Raman measurements are presented in  $\text{Bi}_4\text{Ge}_3\text{O}_{12}$ . The signal-to-noise using the double Michelson technique is comparable to previously described methods with the added advantage of arbitrarily long pump-probe time delays.

## 1. Introduction

Spectral interferometry is a commonly used technique in ultrafast optical pump-probe experiments. After initial explorations by Kobayashi *et al.* [1–3], it has been employed in measurements of the optical Kerr effect [4–6], rotational and rovibrational dynamics in gases [7], impulsive stimulated Raman scattering (ISRS) [8], field ionization [9], and transient phase spectroscopy [10–12]. It also forms the basis of many optical 2D spectroscopy techniques [13,14]. Some of these applications require or benefit from the possibility of long time delays between the pump pulse and the probe pulse. But in the most straightforward technique, based on producing probe and reference pulses with a Michelson interferometer, the time between pulses is limited by spectrometer resolution. As a result, a Sagnac interferometer has often been used when long time delays are required [1]. In contrast to the methods mentioned above which rely on temporal separation of the probe and reference, we demonstrate a practical alternative technique using two slightly misaligned Michelson interferometers to achieve spatial separation of our probe and reference beams which enables arbitrarily long pump-probe time delays.

Spectral interferometry requires two pulses to be generated, with one pulse serving as a clean reference that is used to measure the spectral phase of the other pulse. Depending on the repetition rate of the laser, spectral interferograms can be recorded pulse-by-pulse, but it is advantageous to average many together, so relative phase stability over a few seconds is needed. In a pump-probe experiment, the pump pulse must not affect the reference pulse or artifacts will appear in the spectral phase and amplitude extracted from the interferogram. A technique

must then arrange for the reference pulse to not overlap the pump pulse using either spatial or temporal separation. In principle, a Mach-Zehnder interferometer achieves this, but because the probe and reference beams propagate along different paths, this scheme is susceptible to air currents and vibrations and requires day-to-day effort to keep it aligned when changing samples. Michelson interferometers produce two pulses with an adjustable time delay and have the advantages of easy alignment and compactness. Compactness helps stability, as only within the interferometer is the beams' relative phase stability affected by vibrations and air currents. However, the co-propagation of the pulses makes spatial separation of the probe and reference pulses impossible, so temporal separation is required. The pump pulse must arrive between the reference and probe pulses in time, and the need to resolve the spectral interference fringes means that the maximum temporal separation is typically on the order of picoseconds. For the broadband supercontinuum used in this experiment, our spectral resolution corresponds to a maximum separation of less than 1 ps between the probe and reference pulses.

Misawa and Kobayashi previously showed that a Sagnac interferometer can be used to measure phase and amplitude spectra over long time delays [1]. In a Sagnac interferometer scheme, the probe and reference pulses counterpropagate through the sample. By placing the sample near the beamsplitter of the interferometer, a large time delay is achieved between the reference and the probe beam when they pass through the sample [14,15]. The maximum time delay achievable with a Sagnac interferometer depends on its length. Using the Sagnac interferometer, Wilson *et al.* demonstrated impulsive stimulated Raman scattering [8], while a more recent implementation by Hotchkiss *et al.* [12] achieved phase spectroscopy with a better signal-to-noise ratio than [1]. Here, we introduce an alternative technique that separates the probe and reference beams spatially at the sample using two slightly misaligned Michelson interferometers. Like the Sagnac interferometer, our technique is mostly common path, but with added advantages of: easy alignment, continuously adjustable probe/reference time delay and full polarization control. The setup can be conveniently switched between standard transient absorption (TA) spectroscopy and simultaneous transient amplitude/phase spectroscopy.

## 2. Experiment

A Yb:KGW laser (Light Conversion Carbide [16]) with central wavelength 1030 nm and 200 fs pulse duration is used to produce pump and probe beams. The laser repetition rate is set to 3 kHz. Half of the 1030 nm laser output pumps an optical parametric amplifier (OPA, Light Conversion Orpheus [16]), the signal output of which (or its second harmonic) is the pump beam. We use a mechanical chopper synchronized to the laser repetition rate to block two out of every four laser shots in the pump beam path. A small part of the 1030 nm laser output is split off before the OPA and used to generate supercontinuum in a water cell. This 1030 nm beam has an adjustable delay for the pump-probe experiment. A dielectric mirror (CVI TLM1-1030-0 [16]) is used to separate the fundamental at 1030 nm from the visible supercontinuum. A camera (Princeton Instruments ProEM [16]) records spectra at 3 kHz. A diagram of the phase-sensitive pump-probe setup is illustrated in Fig. 1. Before it is directed to the sample, we split the supercontinuum into co-propagating probe and reference pulses using a Michelson interferometer (labeled M1). The interferometer is constructed using a beam splitter (Thorlabs BSS10 [16], which has approximately 50% reflectivity over a broad spectrum for s-polarized light) a dispersion-compensating window (Thorlabs BCP4310 [16]), and protected silver mirrors. Propagation of the broadband supercontinuum in the water cell and glass results in group delay dispersion of approximately 1300 fs<sup>2</sup>, resulting in a wavelength-dependent pump-probe time delay.

With one interferometer, the spectral interferograms measured by the camera are

$$I_1(\omega) \propto |E_{\text{ref}}(\omega)|^2 + |E_{\text{pr}}(\omega)|^2 + 2|E_{\text{ref}}(\omega)||E_{\text{pr}}(\omega)| \cos[\omega\tau_1 + \phi_{\text{pr}}(\omega) - \phi_{\text{ref}}(\omega)], \quad (1)$$

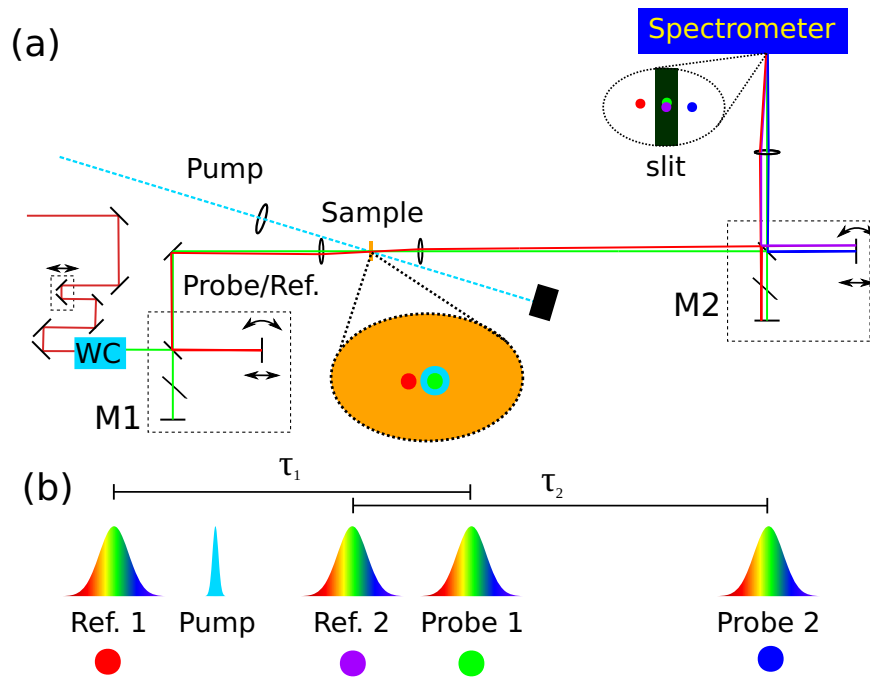


**Fig. 1.** (a) Diagram of the experiment. A broadband supercontinuum is generated using a delayable 1030 nm pulse in a water cell (WC). A Michelson interferometer (M1) splits the probe supercontinuum into reference and probe pulses. The interferometer is slightly misaligned so that the reference beam does not pass through the same spot on the sample as the probe beam, as shown in the central inset. The pump beam (shown in cyan) overlaps with the probe spot but not the reference spot (shown in red). A second Michelson interferometer (M2) compensates for the misalignment of M1 so that fringes are observed. The upper right inset shows the position of the four output beams (each has been assigned a unique color) at the spectrometer slit when the two interferometers have been purposely misaligned. (b) Schematic showing the temporal sequence of pulses at the spectrometer entrance plane.

where  $E_{\text{ref}}$  is the reference electric field,  $E_{\text{pr}}$  is the probe electric field, and  $\tau_1$  is the time delay between pulses from the relative optical path difference within M1. Using Fourier techniques, the interference term can be isolated and the relative spectral phase  $\phi_{\text{pr}}(\omega) - \phi_{\text{ref}}(\omega)$  can be extracted [17]. This scheme has been used to measure the optical Kerr nonlinearity in transparent media [4] and is especially effective in gases [5]. However, as mentioned before, when the time delay between the pump and probe pulses is longer than the time delay between the probe and reference pulses, the response of the medium to the pump pulse can affect the reference pulse too, resulting in the distortion and/or cancellation of the measured spectral phase. There is unfortunately a strong constraint on the maximum achievable  $\tau_1$ . The spectral fringe spacing is  $1/\tau_1$ , so as  $\tau$  increases, the spectral fringes become finer and finer. As the fringe spacing approaches the finite resolution of the spectrometer, fringe visibility is reduced and eventually lost. Thus, there is a maximum achievable time delay  $\tau_{\text{res}}$ . In our case, we use a grating with 300 grooves per mm in order to capture a large bandwidth, and  $\tau_{\text{res}} \approx 800$  fs.

To overcome this time delay limit, we add a second identical interferometer (labeled M2 in Fig. 1) after the probe propagates through the sample and is collimated. As depicted in Fig. 1(b), the second interferometer produces a replica of both probe and reference pulses. The

interferogram is now

$$\begin{aligned}
 I_2(\omega) \propto & |E_{\text{ref},1}(\omega)|^2 + |E_{\text{ref},2}(\omega)|^2 + |E_{\text{pr},1}(\omega)|^2 + |E_{\text{pr},2}(\omega)|^2 \\
 & + 2|E_{\text{ref},1}(\omega)||E_{\text{ref},2}(\omega)| \cos[\omega\tau_2 + \phi_{\text{ref},1}(\omega) - \phi_{\text{ref},2}(\omega)] \\
 & + 2|E_{\text{pr},1}(\omega)||E_{\text{pr},2}(\omega)| \cos[\omega\tau_2 + \phi_{\text{pr},1}(\omega) - \phi_{\text{pr},2}(\omega)] \\
 & + 2|E_{\text{ref},1}(\omega)||E_{\text{pr},1}(\omega)| \cos[\omega\tau_1 + \phi_{\text{ref},1}(\omega) - \phi_{\text{pr},1}(\omega)] \\
 & + 2|E_{\text{ref},2}(\omega)||E_{\text{pr},2}(\omega)| \cos[\omega\tau_1 + \phi_{\text{ref},2}(\omega) - \phi_{\text{pr},2}(\omega)] \\
 & + 2|E_{\text{ref},1}(\omega)||E_{\text{pr},2}(\omega)| \cos[\omega(\tau_1 + \tau_2) + \phi_{\text{ref},1}(\omega) - \phi_{\text{pr},2}(\omega)] \\
 & + 2|E_{\text{ref},2}(\omega)||E_{\text{pr},1}(\omega)| \cos[\omega(\tau_1 - \tau_2) + \phi_{\text{ref},2}(\omega) - \phi_{\text{pr},1}(\omega)],
 \end{aligned} \tag{2}$$

where  $\tau_2$  is the time delay between pulses from M2. We can now increase  $\tau_1$ , which determines the maximum pump-probe time delay. Provided  $|\tau_1 - \tau_2| < \tau_{\text{res}}$ , the last term produces observable fringes between the probe and reference pulses, and if  $\tau_1$  and  $\tau_2$  are both large compared with  $\tau_{\text{res}}$ , no fringes from the other terms can be resolved. Introducing the second interferometer results in a reduction in transmitted power. It also reduces fringe visibility, because only two of the four pulses impinging on the spectrometer produce interference fringes. Since the supercontinuum typically must be attenuated to avoid saturating the camera, the loss of transmitted power is not a large concern. The loss of fringe visibility reduces the signal-to-noise ratio, but the advantage of going to long time delays outweighs this for many applications. It should be noted that the probe-reference delay does not need to be changed during the pump-probe scans: once it is set and fringes are optimized, it need not be adjusted for the duration of an experiment.

With the second interferometer, we can increase the maximum pump-probe delay to approximately 30 ps, limited only by the range of motion of the translation stages in the interferometers. Crucially though, the second interferometer allows us to bypass the spectral resolution issue altogether. Tilting one of the mirrors in the first interferometer by an angle  $\theta$  produces a displacement of the probe and reference beams at the sample. Now the pump pulse does not affect the reference pulse because they do not overlap *spatially*. For a path length  $x_1$  between the tilted mirror and the focusing lens, the reference beam is offset on the focusing lens by  $\theta x_1$  and is offset on the sample by  $\theta f$ , where  $f$  is the focal length of the lens. This misalignment moves the reference spot off the spectrometer entrance slit. To restore the spectral fringes, we misalign the second interferometer in the opposite way, which has the effect of moving reference beam 2 back onto the entrance slit. The misalignment results in reference beam 1 and probe beam 2 being blocked by the spectrometer entrance slit, as shown in the upper right inset of Fig. 1(a). The interferogram is now simply

$$\begin{aligned}
 I_{2,\text{mis}}(\omega) \propto & |E_{\text{ref},2}(\omega)|^2 + |E_{\text{pr},1}(\omega)|^2 \\
 & + 2|E_{\text{ref},2}(\omega)||E_{\text{pr},1}(\omega)| \cos[\omega(\tau_1 - \tau_2) + \phi_{\text{ref},2}(\omega) - \phi_{\text{pr},1}(\omega)],
 \end{aligned} \tag{3}$$

restoring the fringe visibility. With this ‘‘compensated misalignment’’ technique, we are able to measure at time delays limited only by the length of our pump-probe delay stage.

### 3. Results

We exhibit the double Michelson scheme on two femtosecond spectroscopy techniques that depend on long pump-probe time delays: transient phase spectroscopy and impulsive stimulated Raman scattering (ISRS) spectroscopy.

#### 3.1. Transient phase spectroscopy

Related to transient absorption (TA) spectroscopy by a Kramers-Kronig transformation [11], transient phase (TP) spectroscopy is the measurement of the time-dependent probe phase shift as

a function of probe photon energy. For the measurement of some phenomena, TP spectroscopy has advantages over TA [12]. It was recently found that refractive index changes can cause artifacts in pump-probe measurements of polariton dynamics [18], and direct measurements of the amplitude and phase may allow these effects to be more reliably disentangled.

Figure 2 displays TA (Fig. 2(a)) and TP (Fig. 2(b)) data for a tetracene film with pump-probe time delay up to 5 ns using a pump wavelength of 470 nm. Tetracene films (200 nm) were thermally evaporated onto quartz substrates at a base pressure of  $< 5 \times 10^{-5}$  Pa connected to an  $N_2$  purged glovebox ( $< 1$  ppm  $H_2O$ ,  $O_2$ ). The material was evaporated from a quartz crucible with an evaporation rate of 0.2 nm/s. The sample was then transferred to an  $N_2$  purge cell for optical measurements. For this experiment, the probe beam was focused using a curved silver mirror (focal length 10 cm) and the pump beam was focused using a 30 cm focal length lens. After the sample, the probe beam was collimated using a 10 cm focal length achromat lens, sent through the second Michelson interferometer, and finally focused on the entrance slit of the spectrometer using a curved silver mirror (focal length 10 cm).

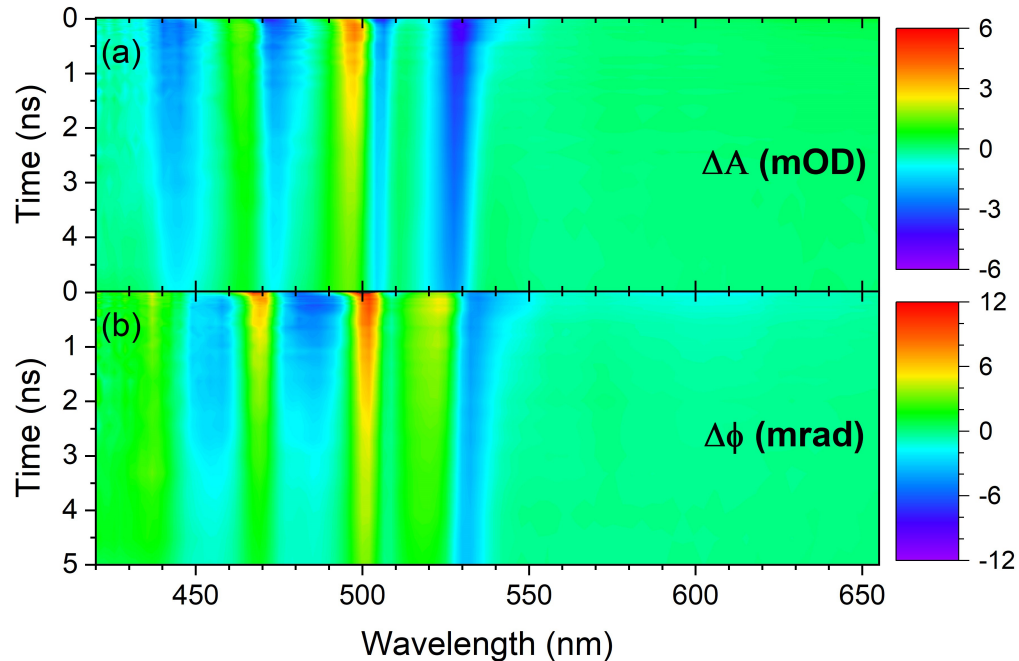


**Fig. 2.** Measured (a) transient absorbance and (b) transient phase shift as a function of wavelength and time delay for a 200 nm tetracene film.

The TA spectrum is consistent with previous results on similar samples [19] while careful analyses of the excited state kinetics can be found elsewhere [19,20]. No polarization dependence was observed, indicating that the sample is isotropic on the spatial scale of the laser spots. At each time delay, average pump-on and pump-off interferograms are calculated. Denoting values from the pump-on interferogram with prime (e.g.  $E'_{pr}$  is the probe field with the pump unblocked and  $E_{pr}$  is the probe field with the pump blocked), we extract  $|E'_{pr,1}(\omega)|$ ,  $|E_{pr,1}(\omega)|$ ,  $\phi_{ref,2}(\omega) - \phi'_{pr,1}(\omega)$  and  $\phi_{ref,2}(\omega) - \phi_{pr,1}(\omega)$  from the interferograms using standard techniques [17]. The transient absorbance spectrum is  $\Delta A(\omega) = (|E'_{pr}(\omega)|^2 - |E_{pr}(\omega)|^2)/|E_{pr}(\omega)|^2$ , and the transient phase shift spectrum is  $\Delta\phi(\omega) = \phi'_{pr}(\omega) - \phi_{pr}(\omega)$ .

For the scan shown in Fig. 2, we averaged 50000 spectra (17 seconds) per time delay. Absorbance and phase spectra at four time delays from this data set are shown in Fig. 3. We

generated statistical error bars by partitioning the data into 20 intervals and calculating the standard deviation of the phase and amplitude for each wavelength and time. The width of each line in Fig. 3 indicates the standard deviation of the mean value of  $\Delta A$  or  $\Delta\phi$ . The uncertainty in  $\Delta A$  and  $\Delta\phi$  is greater for shorter wavelengths because the probe spectral intensity is smaller on that side of the spectrum due to increased absorption by the tetracene film.

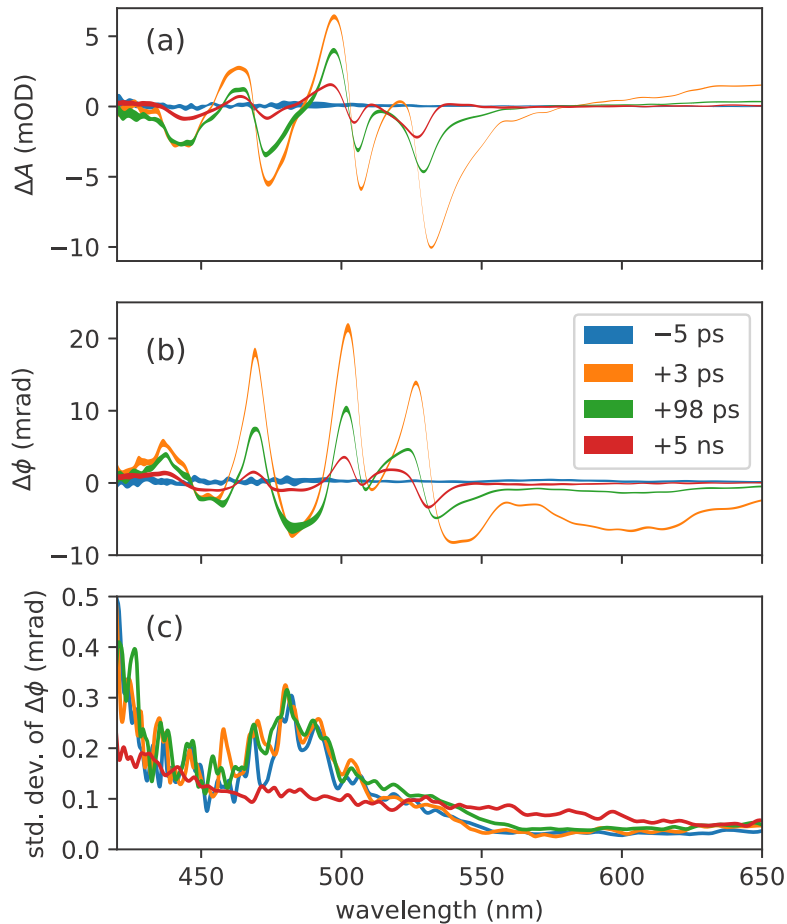


**Fig. 3.** Absorbance (a) and phase shift (b) spectra for the 200 nm tetracene film at four pump-probe time delays:  $-5$  ps (blue),  $+3$  ps (orange),  $+98$  ps (green), and  $+5$  ns (red). (c) The standard deviation of the mean of  $\Delta\phi(\omega)$  calculated using 50000 spectra.

Because phase noise performance is central to this paper, we directly compared our noise level to a recent measurement by Tanghe *et al.* [21], who reported a phase uncertainty value of 0.29 mrad for 2 seconds averaging using a single Michelson interferometer with probe/reference separation (and hence pump/probe delay) limited to  $t \leq 2$  ps. Using the data set of Fig. 2 but restricting the average to 6000 shots (2 seconds), we observe a similar phase standard deviation of 0.27 mrad near 600 nm. In addition to the experimental approach (dual Michelson interferometers reported here), stability involves specific local factors such as vibration isolation, room temperature stability, room air currents, and quality of optics. Our experiments were done on an optical table that was not floated; the optical path was not enclosed or protected from room air currents and temperature fluctuations; and the optical components were common quality (e.g., Thorlabs standard mirror mounts KMS and KM100 [16]). With more attention to details,

it is possible that our phase stability could have been improved. On the other hand, it may be dominated by other noise sources, for example from the camera. In any case, the phase stability was sufficient to achieve similar results to Tanghe *et al.* [21].

We have also measured phase spectra of laser dyes. As in [12], we find good agreement between the phase spectrum measured and that calculated from the absorbance spectrum via a Kramers-Kronig transformation.

### 3.2. Impulsive stimulated Raman scattering

Pump-probe techniques can have advantages over continuous wave techniques for Raman spectroscopy, particularly for very low frequency phonon modes [22]. Detection by a chirped probe pulse is also sometimes done in multidimensional Raman spectroscopy [23]. In transparent media, where Raman scattering is nonresonant, coherent phonons primarily produce a phase shift of the probe pulse [15,24]. Spectral interferometry measurements of the phonon-induced phase shift were demonstrated by Wilson *et al.* [8]. Achieving optimal spectral resolution in a coherent phonon experiment requires long pump-probe time delays, though a technique based on a synthetic temporal aperture was developed to get around this requirement while still using a Michelson interferometer [25]. To demonstrate the ability of our technique to do nonresonant impulsive stimulated Raman scattering, we measured bismuth germanate ( $\text{Bi}_4\text{Ge}_3\text{O}_{12}$  or BGO), which has a long-lived A symmetry phonon with a large amplitude near 2.7 THz. Our sample is a (001) oriented, 0.5 mm thick crystal (MTI [16]).

Results are shown in Fig. 4. For this experiment the pump beam was centered at 760 nm and a tight focusing geometry was employed to minimize pump-probe walkoff inside the crystal due to group velocity mismatch. A microscope objective was used to focus both the pump and probe

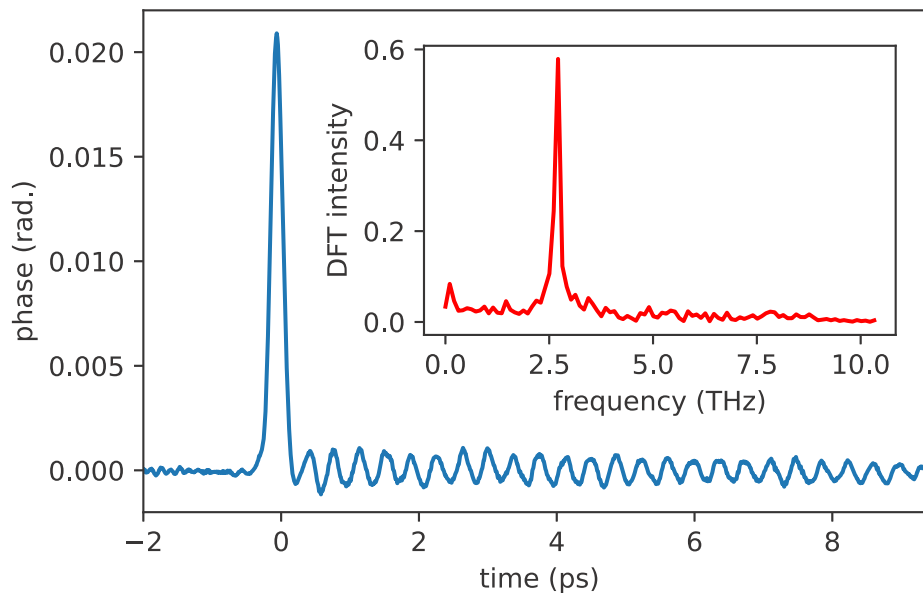


**Fig. 4.** Measured phase shift and optical Kerr response (spike near zero delay) in bismuth germanate (BGO) using the double Michelson technique. In this material, the ISRS response in the near infrared to visible is independent of wavelength. The time-dependent phase shift is constructed from data taken as a function of pump-probe time delays. The inset shows the discrete Fourier transform of the time-dependent signal, yielding a peak at 2.7 THz, the expected frequency of the strongest low frequency A symmetry phonon in BGO.

beams onto the sample. The frequency domain pump-induced phase and amplitude change was transformed to the local probe pulse time axis by a discrete Fourier transform, which requires knowledge of the probe pulse's spectral chirp [4]. We averaged 10000 frames at each time delay before extracting the phase. Due to our use of a 200 fs pump pulse, we did not observe modes with higher frequency than 2.7 THz in BGO.

Figure 4 shows delays up to 9 ps. We emphasize that with a single interferometer, we would not be able to measure the coherent phonon response at time delays longer than 1 ps due to the limit set by the resolution of the spectrometer, because the phase shift of the probe pulse would be distorted by the phase shift of the reference pulse. It would be enhanced if the probe-reference time delay is set to one half the period of the coherent phonon [25]. While this condition can be achieved for one mode at a time, it becomes less practical if there is more than one mode in the spectrum. Here, as in [8], the reference pulse is not affected by the pump pulse, in our case because there is no spatial overlap.

#### 4. Conclusion

In summary, we have demonstrated a novel double Michelson technique for pump-probe spectral interferometry at long time delays. We used it to perform sensitive measurements of transient phase and absorption spectra in a tetracene film. We also used it to perform phase-sensitive ISRS measurements of coherent phonons in bismuth germanate (BGO). It has a number of practical advantages over a Sagnac interferometer. Switching between a phase-sensitive probe measurement and standard transient absorption spectroscopy is done simply by blocking the reference arm of the first Michelson interferometer. The time delay between probe and reference pulses is continuously adjustable.

The capability of this technique to measure at long time delays with easy-to-use and relatively stable Michelson interferometers will have application in other contexts, including measurement of rotational wavepacket revivals [7], rotational permanent alignment [26], and time-resolved spectroscopy of laser-excited plasmas.

**Funding.** Physical Measurement Laboratory (70NANB22H088).

**Acknowledgments.** We acknowledge support from the National Institute of Standards and Technology/National Research Council Research Associateship Program (C. D. C.). S. E. acknowledges support from the U.S. Department of Commerce, National Institute of Standards and Technology under the financial assistance award 70NANB22H088. The authors thank Jagannath Paul for technical assistance.

**Disclosures.** The authors declare no conflict of interest.

**Data availability.** Data underlying the results presented in this paper are not publicly available at this time but may be obtained from the authors upon reasonable request.

#### References

1. K. Misawa and T. Kobayashi, "Femtosecond Sagnac interferometer for phase spectroscopy," *Opt. Lett.* **20**(14), 1550–1552 (1995).
2. E. Tokunaga, A. Terasaki, and T. Kobayashi, "Femtosecond phase spectroscopy by use of frequency-domain interference," *J. Opt. Soc. Am. B* **12**(5), 753–771 (1995).
3. E. Tokunaga, A. Terasaki, and T. Kobayashi, "Femtosecond continuum interferometer for transient phase and transmission spectroscopy," *J. Opt. Soc. Am. B* **13**(3), 496–513 (1996).
4. K. Y. Kim, I. Alexeev, and H. M. Milchberg, "Single-shot supercontinuum spectral interferometry," *Appl. Phys. Lett.* **81**(22), 4124–4126 (2002).
5. Y.-H. Chen, S. Varma, I. Alexeev, and H. Milchberg, "Measurement of transient nonlinear refractive index in gases using xenon supercontinuum single-shot spectral interferometry," *Opt. Express* **15**(12), 7458–7467 (2007).
6. J. K. Wahlstrand, Y.-H. Cheng, and H. M. Milchberg, "Absolute measurement of the transient optical nonlinearity in N<sub>2</sub>, O<sub>2</sub>, N<sub>2</sub>O, and Ar," *Phys. Rev. A* **85**(4), 043820 (2012).
7. Y.-H. Chen, S. Varma, A. York, and H. M. Milchberg, "Single-shot, space- and time-resolved measurement of rotational wavepacket revivals in H<sub>2</sub>, D<sub>2</sub>, N<sub>2</sub>, O<sub>2</sub>, and N<sub>2</sub>O," *Opt. Express* **15**(18), 11341–11357 (2007).
8. J. W. Wilson, P. Schlup, and R. Bartels, "Phase measurement of coherent Raman vibrational spectroscopy with chirped spectral holography," *Opt. Lett.* **33**(18), 2116–2118 (2008).

9. J. K. Wahlstrand, S. Zahedpour, A. Bahl, M. Kolesik, and H. M. Milchberg, "Bound-electron nonlinearity beyond the ionization threshold," *Phys. Rev. Lett.* **120**(18), 183901 (2018).
10. T. Fuji, T. Yoda, T. Hattori, and H. Nakatsuka, "Phase Sensitive Pump-Probe Spectroscopy Using a Michelson-Type Interferometer," *Jpn. J. Appl. Phys.* **39**(4R), 1738 (2000).
11. H. Kano and T. Kobayashi, "Simultaneous measurement of real and imaginary parts of nonlinear susceptibility for the verification of the Kramers–Kronig relations in femtosecond spectroscopy," *Opt. Commun.* **178**(1-3), 133–139 (2000).
12. R. R. Tamming, J. M. Hodgkiss, and K. Chen, "Frequency domain interferometry for measuring ultrafast refractive index modulation and surface deformation," *Adv. Phys.: X* **7**(1), 2065218 (2022).
13. T. Zhang, C. Borca, X. Li, and S. Cundiff, "Optical two-dimensional Fourier transform spectroscopy with active interferometric stabilization," *Opt. Express* **13**(19), 7432–7441 (2005).
14. T. L. Courtney, S. D. Park, R. J. Hill, B. Cho, and D. M. Jonas, "Enhanced interferometric detection in two-dimensional spectroscopy with a Sagnac interferometer," *Opt. Lett.* **39**(3), 513–516 (2014).
15. J. K. Wahlstrand, R. Merlin, X. Li, S. T. Cundiff, and O. E. Martinez, "Impulsive stimulated Raman scattering: comparison between phase-sensitive and spectrally filtered techniques," *Opt. Lett.* **30**(8), 926–928 (2005).
16. Certain commercial equipment, instruments, or materials are identified in this paper to foster understanding. Such identification does not imply recommendation or endorsement by the National Institute of Standards and Technology, nor does it imply that the materials or equipment identified are necessarily the best available for the purpose.
17. M. Takeda, H. Ina, and S. Kobayashi, "Fourier-transform method of fringe-pattern analysis for computer-based topography and interferometry," *J. Opt. Soc. Am.* **72**(1), 156–160 (1982).
18. S. Renken, R. Pandya, K. Georgiou, R. Jayaprakash, L. Gai, Z. Shen, D. G. Lidzey, A. Rao, and A. J. Musser, "Untargeted effects in organic exciton–polariton transient spectroscopy: A cautionary tale," *J. Chem. Phys.* **155**(15), 154701 (2021).
19. E. M. Grumstrup, J. C. Johnson, and N. H. Damrauer, "Enhanced Triplet Formation in Polycrystalline Tetracene Films by Femtosecond Optical-Pulse Shaping," *Phys. Rev. Lett.* **105**(25), 257403 (2010).
20. J. J. Burdett, D. Gosztola, and C. J. Bardeen, "The dependence of singlet exciton relaxation on excitation density and temperature in polycrystalline tetracene thin films: Kinetic evidence for a dark intermediate state and implications for singlet fission," *J. Chem. Phys.* **135**(21), 214508 (2011).
21. I. Tanghe, J. Butkus, K. Chen, R. R. Tamming, S. Singh, Y. Ussembayev, K. Neyts, D. van Thourhout, J. M. Hodgkiss, and P. Geiregat, "Broadband Optical Phase Modulation by Colloidal CdSe Quantum Wells," *Nano Lett.* **22**(1), 58–64 (2022).
22. R. A. Bartels, D. Oron, and H. Rigneault, "Low frequency coherent Raman spectroscopy," *JPhys Photonics* **3**(4), 042004 (2021).
23. G. Fumero, C. Schnedermann, G. Batignani, T. Wende, M. Liebel, G. Bassolino, C. Ferrante, S. Mukamel, P. Kukura, and T. Scopigno, "Two-Dimensional Impulsively Stimulated Resonant Raman Spectroscopy of Molecular Excited States," *Phys. Rev. X* **10**(1), 011051 (2020).
24. R. Merlin, "Generating coherent THz phonons with light pulses," *Solid State Commun.* **102**(2-3), 207–220 (1997).
25. J. W. Wilson, P. Schlup, and R. A. Bartels, "Synthetic temporal aperture coherent molecular phase spectroscopy," *Chem. Phys. Lett.* **463**(4-6), 300–304 (2008).
26. Y. Feng, H. Pan, J. Liu, C. Chen, J. Wu, and H. Zeng, "Direct measurement of field-free molecular alignment by spatial (de)focusing effects," *Opt. Express* **19**(4), 2852–2857 (2011).